CONTINUOUS DYNAMIC MONITORING TO ENHANCE THE KNOWLEDGE OF A HISTORIC BELL-TOWER

Carmelo Gentile[1*], Antonello Ruccolo[2], Antonella Saisi[1]

[1]*Politecnico di Milano, Milan, Italy*
Department of Architecture, Built environment and Construction engineering (ABC)
Piazza Leonardo da Vinci, 32 – 20133 Milan, Italy
[*]e-mail: carmelo.gentile@polimi.it

[2]*PhD Candidate, PhD_ABC, Politecnico di Milano, Milan, Italy*
Piazza Leonardo da Vinci, 32 – 20133 Milan, Italy

ABSTRACT

The results of the long-term vibration monitoring program, carried out on the bell-tower of *Santa Maria del Carrobiolo* in Monza (Italy), are reported in the paper. The dynamic monitoring was motivated by the weak structural layout of the historic building, with two fronts of the tower being supported by the load-bearing structures of the apse and South aisle of the adjacent church. Furthermore, closely spaced modes with similar mode shapes were clearly identified from ambient vibration tests, hence, the modal parameters of the bell-tower significantly differ from those obtained in past experimental studies of similar masonry structures.
The continuous dynamic monitoring was mainly aimed at enhancing the knowledge of the historic structure, checking the possible evolution of the key resonant frequencies and assessing the effects of changing temperature on the dynamic characteristics of the bell-tower. The main results of the dynamic monitoring for a period of two years highlight distinctive behaviour of the bell-tower, such as the frequency veering exhibited by the lower modes with increased temperature. Subsequently, in order to mitigate the effects of the environmental factors on resonant frequencies, the application of the multiple linear regression (MLR) and the principal component analysis (PCA) tools have been investigated.

Keywords: Automated modal identification; building phases; closely spaced modes; environmental effects; frequency veering; masonry towers.

1. INTRODUCTION

The assessment of ancient masonry towers is a challenging multidisciplinary activity, involving different tasks. It is generally agreed (see e.g. Binda et al. 2000, Lourenço 2006) that a correct approach must not disregard accurate evaluation of building geometry through topographic survey, historic/documentary research and direct (on-site) inspections. Based on those steps, important information are made available on the geometrical layout, the probable building techniques and construction phases, the sequence of transformations and repairs as well as the mapping of discontinuities and damage. Since towers are generally sensitive to ambient excitation, such as micro-tremors and wind, dynamic tests in operational conditions are becoming more popular (see Diaferio et al. 2018 for a list of recent studies reported in the literature) as part of the assessment process. In fact, merging the information collected by historic/architectural research and dynamic investigation – driven by a comprehensive interpretation of the results – should allow also to solve the main uncertainties in establishing numerical models (see e.g. Gentile and Saisi 2007, Ramos et al. 2010, Pena et al. 2010, Oliveira et al. 2012, Tomaszewska and Szymczak 2012, Gentile et al. 2015, Cavalagli et al. 2018, Azzara et al. 2018) and to assess the structural state of preservation of the building in a fully non-destructive and rather quick way.

Although the cantilever-like dynamic behaviour of ancient towers allows the successful monitoring of the resonant frequencies from the data continuously collected by a few sensors (which are permanently installed in the upper part of the building), the idea of implementing vibration-based and cost-effective Structural Health Monitoring (SHM, i.e. the continuous interrogation of sensors installed in the structure aimed at extracting features which are representative of the current state of structural health) for the condition-based maintenance of historic towers has been taking shape recently (Ramos et al. 2010, Cabboi 2013, Cantieni 2014, Gentile et al. 2016, Ubertini et al. 2018, Lorenzoni et al. 2018). Even if especially the temperature turned out to be a dominant driver of modal frequency changes in masonry towers (see e.g. Ubertini 2017), recent post-earthquake

experiences on ancient towers (Gentile et al. 2016, Ubertini et al. 2018, Lorenzoni et al. 2018) clearly highlighted the effectiveness of resonant frequencies as features sensitive to the onset of small structural changes or damages.

The paper mainly focuses on the results of the continuous dynamic monitoring program performed on the bell-tower belonging to the historic complex of *Santa Maria del Carrobiolo* in Monza, Italy (Magnani Pucci et al. 1997). A pre-diagnostic survey of the bell-tower (Saisi et al. 2018) highlighted that the load-bearing walls of the apse and South aisle of the neighbouring church directly support two sides of the tower.

The structural arrangement of the bell-tower, not identified before, appears weak deserving further investigation to assess the actual performance of the structure under permanent loads and exceptional events, like winds and particularly earthquakes. Hence, an extended investigation program, still in progress, was planned to verify the structural behaviour of the tower (Saisi et al. 2018): (a) on-site survey of the geometry and of the building characteristics, as well as of damage/decay visible on the fronts; (b) static monitoring of the more relevant cracks at various levels of the bell-tower by 10 displacement transducers and 5 temperature sensors; (c) ambient vibration tests, aimed at estimating the dynamic characteristics of the structure using operational modal analysis; (d) installation of a dynamic monitoring system to continuously trace the evolution of the resonant frequencies of the tower. The long-term vibration monitoring was mainly aimed at enhancing the knowledge of the historic structure, checking the possible evolution of the key resonant frequencies and assessing the effects of changing temperature on the dynamic characteristics of the bell-tower.

After a concise description of the tower and a summary of selected evidences provided by direct survey and historic research (Section 2), the paper reports the baseline dynamic characteristics estimated from ambient vibration data (Section 3). Subsequently (Section 4), details are given on the monitoring devices and the automated tools adopted to extract the modal parameters from continuously collected time series. Selected results obtained

during two years of continuous monitoring (Section 5) revealed distinctive behaviour of the bell-tower, which conceivably results from the structural arrangement of the building, as well as from the different effects of the changing temperature on the resonant frequencies of the various modes.

At last (Section 6), both supervised (multiple linear regression, Mason et al. 2003) and unsupervised (principal component analysis, Jolliffe 2002) algorithms were applied – with SHM purposes – to remove/mitigate the masking effects induced by the temperature changes on the identified modal frequencies.

2. THE *SANTA MARIA DEL CARROBIOLO* BELL-TOWER

The ancient religious monastery of *Santa Maria del Carrobiolo* (Magnani Pucci et al 1997) was built in different times, clustering former buildings and new structures. At present, it is composed by several buildings: the church and the bell-tower (Fig. 1a), the friary, the hostel, the theatre and other buildings related to the educational activities of the Barnabite religious community. The bell-tower (Fig. 1a) is 33.7 m high and its plan is almost square (5.9 m × 5.7 m, Fig. 1b); the thickness of the masonry walls ranges from 70 cm, at the base level, to 58 cm at the floor below the elegant belfry.

Historical documents testify that the church and the monastery existed since the 13th century, whereas the tower was completed in 1339 (Fig. 1b). The sequence of the construction stages has been confirmed by visual inspection of the masonry discontinuities (Figs. 1-3): (a) the masonry structures of the apse and the right aisle of the church bear the North and West fronts of the bell-tower; (b) the South and East fronts of the tower seems homogeneous from the base to the top and do not exhibit any mechanical connections with the walls of the church (Figs. 1c, 2 and 3a). Moreover, several cracks cut the masonry section and are especially concentrated in the four sides of the floor below the belfry (Fig. 3a). It is worth mentioning that (Fig. 3b) the opening of a deep crack on the West side is opposed by the presence of one metallic tie-rod.

As previously pointed out, the North and West sides of the tower turned out to be directly

supported by the load-bearing walls of the neighbouring church; of course, the detection of this weak structural arrangement from the construction sequence caused concern about the actual structural performance of the bell-tower.

It should be mentioned that a few months before the pre-diagnostic survey, an under-ground car park was built, adjacent to the tower, and its construction caused the re-opening of cracks already repaired and thin cracks appeared on the plaster at the base of the tower after the wall painting. Consequently, a static monitoring system was installed in the tower on June 2014 (Saisi et al. 2018) and consists of 10 displacement transducers, integrated by 5 temperature sensors. The displacement transducers, installed on the main cracks and discontinuities, are linear potentiometers with a maximum stroke of 25 mm and a maximum error on the linearity of 0.2%.

As discussed in (Saisi et al. 2018), the measured opening of cracks turned out to be dominated by thermal effects. In more details, the time variation of measured displacement and temperatures exhibited a regular trend, with periodic repetition of the crack opening measured in similar temperature conditions, so that possible settlements at the foundation level could have been almost negligible.

3. DYNAMIC CHARACTERISTICS OF THE BELL-TOWER

Ambient vibration tests (AVTs) were performed on September 23rd, 2015 (Saisi et al. 2018), with the aim of evaluating the baseline modal parameters of the tower, before permanently installing a dynamic monitoring system in the building.

The dynamic response, sampled at 200 Hz, was acquired at different levels of the tower using high-sensitivity accelerometers (WR 731A, 10 V/g sensitivity and ± 0.50 g peak acceleration) and a multi-channel system with NI 9234 data acquisition modules (24-bit resolution, 102 dB dynamic range and anti-aliasing filters).

Figure 4a shows the arrangement of the accelerometers adopted during the AVT. The data processing, aimed at identifying the modal parameters, was carried out by applying to time

windows of 3600 s both the Frequency Domain Decomposition (FDD, Brincker et al. 2001) and the covariance driven Stochastic Subspace Identification (SSI-Cov, Peeters and De Roeck 1999) techniques.

Table 1 summarizes the modal parameters estimated by applying the two complementary FDD and SSI-Cov methods and the mode classification. Table 1 also compares the corresponding resonant frequencies and scaled modal vectors obtained from the two techniques – through the frequency discrepancy $D_F = |(f_{SSI} - f_{FDD})/f_{SSI}|$ and the Modal Assurance Criterion (MAC, Allemang and Brown 1981) – and highlights an excellent agreement between the two methods in terms of both natural frequencies and mode shapes.

A selected number of identified bending (N-S and E-W) and torsion modes is shown in Fig. 4 (SSI-Cov method). The inspection of Table 1 and Figs. 4b-e reveals unusual dynamic characteristics of the bell-tower, that are conceivably resulting from the peculiar structural layout associated to the building evolution. More specifically, couples of closely-spaced modes with similar mode shapes were observed, so that the sequence of the key vibration modes does not follow the expected series of two bending modes (each one associate to the main planes of a nearly square building) and one torsion mode. The estimated vibration modes include: (a) the first dominant bending mode (f_{x1} = 1.92 Hz, Fig. 4b) in the E-W direction; (b) two bending modes in the N-S plane, with closely-spaced frequencies (f_{y1} = 2.01 Hz and f^*_{y1} = 2.37 Hz) and similar modal deflections shapes (Figs. 4c and 4d); (c) a further mode of dominant bending in the N-S direction (f_{y2} = 4.14 Hz); (d) two torsion modes (f_{T1} = 4.55 Hz and f_{T2} = 5.25 Hz), again with quite similar shapes; (e) the last mode, involving dominant bending in the E-W direction (f_{x2} = 7.53 Hz).

4. MONITORING HARDWARE AND DATA ANALYSIS

Since October 22nd, 2015, the tower dynamic response has been continuously acquired at

200 Hz through (Fig. 5): (a) 4 MEMS accelerometers (Kistler model 8330A3, 1.2 V/g sensitivity, ± 3.00 g peak acceleration, 1.3 μg resolution and 0.4 μg/√Hz rms noise density); (b) one Ethernet carrier with NI 9234 data acquisition module and (c) one local PC for the management of the continuous data recording and storage in single files of 60 min. The monitoring system is installed at the higher available level, despite it would not be the optimum for the estimation of all the modes: during the monitoring, only the modes illustrated in Figs. 4b-e were tracked with good accuracy and high identification rate.

It is further noticed that both the outdoor temperature on the South side of the tower and the indoor temperature at different levels of the structure are measured through 5 thermocouples – denoted as named T_{0N}, T_{1E}, T_{2E}, T_{2W} and T_S in Fig. 5 – so that the temperature conditions within the structure are quite extensively described.

A proprietary software (Busatta 2012) has been developed in the LabVIEW environment to process the acceleration data through the following steps: (a) creation of a database with the original time series (in compact format) for later developments; (b) signal pre-processing (i.e., de-trending and de-spiking of the raw data); (c) detection of the time series containing the swinging of bells and extraction of the related time intervals from each dataset; (d) for each 1-hour dataset, creation of one file including only the ambient vibration data; (e) low-pass filtering and decimation of each "bell-free" dataset (7th order Butterworth low-pass filtering with cut-off frequency of 12.5 Hz and decimation to reduce the sampling frequency from 200 Hz to 25 Hz); (f) reduction of each (low-pass filtered and decimated) time window to the constant length of 3000 s for the application of the output-only modal identification tools.

The extraction of the modal parameters from each 3000 s dataset is performed by applying a fully automated algorithm, based on the SSI-Cov method and developed within a previous research (Cabboi et al. 2017). The adopted procedure involves the two main steps of modal parameters estimation and modal tracking:

- The modal parameters estimation is performed through an automatic interpretation of

the stabilization diagrams (see e.g. Peeters and De Roeck 1999), based on the sensitivity of frequency and mode shape to the model order variation. For each dataset, after having filtered the spurious poles by checking the associated damping ratio and modal complexity value (Reynders et al. 2012), the poles sharing similar frequencies and mode shapes are clustered together, and a set of representative modal parameters (i.e. natural frequency, damping and mode shape) is estimated for each cluster. In the present application: (a) the stabilization diagrams are generated by varying the model order from 20 to 120 and (b) the maximum allowable damping ratio and modal complexity index (Cabboi et al. 2017), adopted in the noise modes elimination step, were set equal to 10% and 0.20, respectively;

- The modal tracking, aimed at providing the time evolution of the parameters of each mode, is based on frequency and MAC variation with respect to a pre-selected list of baseline modes. It is worth mentioning that this step is performed in an adaptive way, i.e. by updating the MAC and frequency variation threshold of each mode after a new dataset has been analyzed.

For the details on the automated modal identification, the interested reader is referred to (Cabboi et al. 2017).

5. CONTINUOUS DYNAMIC MONITORING: RESULTS

This section summarizes the main results of the dynamic monitoring over a time span of two years (i.e., from 22/10/2015 to 21/10/2017). During this time interval, more than 14000 datasets were collected and automatically processed to identify the modal parameters.

The evolution of the hourly averaged value of the temperatures collected during the entire monitoring interval is shown in Figs. 6a and 6b, whereas Table 2 reports the correlation coefficients between the temperature data measured in the first year. The results of Figs. 6a-b and Table 2 show that all temperature data are highly correlated, with the time series of T_{1E}, T_{2E}, and T_{2W} being almost perfectly correlated (as the correlation coefficients are

very close to one). Consequently, only one of those temperatures will be used in the next section to establish a regression model of each frequency.

It is further noticed that, during the second year of monitoring, a long interruption of the temperature monitoring occurred due to the malfunction of the data logger for the automatic acquisition of the temperature sensors and to maintenance operations in the electric cabin providing power to the bell-tower. Similarly, the continuous monitoring of the dynamic responses underwent a much shorter interruption (Fig. 7), associated only to the electric maintenance.

Figure 7 shows the time variation of the automatically identified natural frequencies during the two years of dynamic monitoring, whereas Table 3 summarizes the statistic description of each modal frequency in terms of mean value (f_{ave}), standard deviation (σ_f), and extreme values (f_{min}, f_{max}). It should be noted that the relevant statistics of each frequency are listed in Table 3 for both the first and second year of monitoring. Differently from what reported by Gentile et al. 2016 for the onset of small damage, no significant variations are detected between the two subsequent periods, suggesting that no appreciable change in the structural condition occurred during the monitoring.

The inspection of Fig. 7 and the results of Table 3 suggest the following comments:

(1) Despite the low level of the ambient excitation that generally existed during the monitoring, 4 vibration modes were estimated with high occurrence and accuracy;

(2) The frequency of modes f_{x1} and f_{T2} (Fig. 7) shows remarkable increase, during Spring and Summer periods. Hence, the trend generally observed in previous studies (see e.g. Ramos et al. 2010, Cabboi 2013, Cantieni 2014, Gentile et al. 2016, Ubertini et al. 2017) of ancient masonry towers is confirmed, with the frequency of those modes being strongly affected by the temperature and increasing with increased temperature;

(3) Conversely, the frequency of modes f_{y1} and f^*_{y1} seems to be less sensitive to the environmental changes and exhibits maximum standard deviation in the order of 0.010 and 0.017 Hz, respectively. For those modes, the frequency increase associated to the

thermal expansion and the resulting "compacting" effect is conceivably balanced by the slackening of the tie-rod which strengths the West load-bearing wall and links the North and South front of the tower. This assumption is confirmed by zooming the evolution of temperature and resonant frequency during the Winter season: as shown in Fig. 8, the peaks of the outdoor temperature (T_S) correspond to the valleys (relative minima) of frequencies f_{y1} (Fig. 8a) and f^*_{y1} (Fig. 8b). Hence, the tension force in the tie rod, decreasing with increased temperature, is conceivably one dominant driver of the changes observed in Figs. 7 and 8. In more details, the trend in Fig. 8 suggests that, in the cold seasons, the frequency of modes f_{y1} and f^*_{y1} tends to increase with the increased tension force in the tie-rod (induced by the decreased temperature); on the other hand, in the hot seasons, the loss of tensile force in the tie-rod is balanced by the micro-cracks closing induced by thermal expansion of the materials;

(4) As a consequence of the different effect exerted by the temperature on the frequencies of the lower modes f_{x1} and f_{y1}, those frequencies exhibit crossing during Summer (Fig. 7a). To the best of the authors' knowledge, this behavior has not been documented before for masonry towers. Furthermore, when the crossing of the two frequencies f_{x1} and f_{y1} occurs, the corresponding mode shapes tend to hybridize: in other words, the two modes – which usually involve pure bending in orthogonal planes, as shown in Figs. 4b and 4c 10b– became associated to biaxial bending (in both the main E-W and N-S planes) when the frequencies move closer to each other. Moreover, the mode shape hybridization, indicating a structural phenomenon which is similar to frequency veering (see e.g. Bendettini et al. 2009, Giannini and Sestieri 2016), is more remarkable for mode f_{y1}.

Finally, Fig. 9 shows the correlation between the identified frequencies and the outdoor temperature T_S, along with the best fit line and the coefficient of determination R^2. The plots in Figs. 9a-d refer to a time period (from 01/06/2016 to 21/10/2016) of the first year of monitoring, whereas Figs. 9e-h refer to the corresponding time period (from 01/06/2017 to 21/10/2017) of the second year. The plots in Fig. 9 not only confirm what previously

observed about the effects of temperature on resonant frequencies but also highlight that no clear differences are detected between the corresponding populations of temperature-frequency points. Even the slope of the best fit lines does not exhibit appreciable changes, so that the invariance of temperature-frequency correlation suggests that no significant structural changes occurred in the bell-tower during the two years of continuous monitoring. Of course, it is worth recalling that the resonant frequencies are global parameters, which are directly related to stiffness (and mass) distribution, and the invariance of temperature-frequency correlation does not necessarily imply the invariance of structural strength and safety.

6. REMOVAL OF ENVIRONMENTAL EFFECTS

As shown in the previous section, the environmental factors significantly affect the resonant frequencies of the bell-tower. As SHM strategies commonly use the natural frequencies as features sensitive to structural changes, several procedures have been proposed or applied to improve the resonant frequencies estimate and mitigate the masking effects of environmental factors (see e.g. Ramos et al. 2010, Cabboi 2013, Gentile et al. 2016, Ubertini et al. 2017, Azzara et al. 2018). When the environmental parameters are measured, regression and interpolation analyses might be performed, during a reference time interval (or "training period"), to estimate the relationship between the environmental variables and the observed frequencies. Alternatively, unsupervised learning algorithms, such as the ones based on the principal component analysis (PCA, Jolliffe 2002), could be applied to account for the different unmeasured factors, affecting the modal frequencies during a training period. Both procedures are usually coupled to novelty analysis (Gentile et al. 2016, Ubertini et al. 2018, Azzara et al. 2018) of the frequency residual errors to identify the onset of structural anomalies.

Among the different techniques available in the literature to mitigate the environmental effects, the multiple linear regression algorithm (MLR, see e.g. Mason et al. 2003) has been firstly applied. This choice results from the availability of several measurements of

temperature (Figs. 5 and 6), as well as by the possibility of representing the non-linear dependence of natural frequencies on temperature. More specifically, each response variable y_k (i.e., the *i*-th resonant frequency) at current time *k* has been modelled using a second order polynomial and 3 temperatures T_{0N}, T_{2W} and T_S as predictors (input variables):

$$y_k = \beta_0 + \beta_1 T_{0N,k} + \beta_2 T_{2W,k} + \beta_3 T_{S,k} + \beta_4 (T_{0N,k})^2 + \beta_5 (T_{2W,k})^2 + \beta_6 (T_{S,k})^2 \quad (1)$$

Subsequently, the PCA has been applied to detect and extract the environment effects from the frequency time series. This approach represents an attractive option because it works without any measurement of the environmental parameters and is applied to reduce the dimensions of a data set by retaining the characteristics of the original data mostly contributing to its variance.

By introducing the matrix $\boldsymbol{Y} \in \Re^{n \times N}$, collecting *N* samples of the frequency estimates of *n* vibration modes, the linear mapping into a lower dimension *m* is performed by:

$$\boldsymbol{X} = \boldsymbol{T}\,\boldsymbol{Y} \quad (2)$$

where the scores matrix $\boldsymbol{X} \in \Re^{m \times N}$ contains the principal component scores and $\boldsymbol{T} \in \Re^{m \times n}$ is the loading matrix. As the singular value decomposition of the covariance matrix $\boldsymbol{Y}\boldsymbol{Y}^T$ gives $\boldsymbol{Y}\boldsymbol{Y}^T = \boldsymbol{U}\boldsymbol{\Sigma}^2\boldsymbol{U}^T$, the matrix $\boldsymbol{T}$ can be approximated by retaining the first *m* columns of $\boldsymbol{U}^T$ in order to account for the major part of the original data variance.

Once the reduced dimension *m* is chosen, the predicted frequency matrix $\boldsymbol{Y}^* \in \Re^{n \times N}$ can be estimated through the well-known remapping property of the PCA ($\boldsymbol{Y}^* = \boldsymbol{T}^T\boldsymbol{T}\boldsymbol{Y}$), that allows reconstructing the most significant part of the original data. In the present case (4 frequencies available) the best results have been obtained by retaining m=2 principal components in the linear PCA.

The MLR model and PCA-based regression were estimated using the data collected in the first year of monitoring (i.e., the time interval from 22/10/2015 to 21/10/2016 was assumed as training period) and, subsequently, the resulting approximate relationships were applied to predict (or to clean) the resonant frequencies of the entire monitoring

period.

A comparison of the performance of the two investigated approaches is presented in Fig. 10 through the time evolution of the cleaned observations in the training period. Although at first glance the two procedures seem to provide a similar performance, it should be noticed that the cleaned observations obtained by applying the MLR (Figs. 10a and 10b) still show some correlation, meaning that the influence of common factors was not completely removed. On the other hand, the PCA leads to better cleaned frequencies (Figs. 10c and 10d). The same conclusion is quantitatively confirmed by: (a) inspecting the correlation between the identified and the predicted observation (Fig. 11), for each mode; (b) comparing (Table 4) the predicted and automatically identified resonant frequencies through the coefficient of determination (R^2), the correlation coefficient (ρ_{xy}) and the Loss Function (LF, Ljung 1999).

Finally, the variations of the cleaned modal frequencies (PCA-based regression) in the whole monitoring period are illustrated in Fig. 12.

7. CONCLUSIONS

The paper focuses on the contribution of continuous monitoring to increase the knowledge of a challenging heritage structure and to support the future preservation actions. The interest on the investigated ancient bell-tower of the church of *Santa Maria del Carrobiolo* in Monza (Italy) stems from the weak structural layout, with two fronts being directly borne by the side walls of the apse and South aisle of the neighboring church.

The dynamic response of the tower and the results of 2-years vibration monitoring allow to significantly enhance the knowledge of the global structural behaviour of the building and reveal some unique aspects, which are conceivably related to the unusual structural layout of the tower and to the observed damage pattern:

- Closely spaced modes with similar mode shapes were clearly identified, highlighting dynamic characteristics of the tower which are very different from the ones previously

observed on similar structures. Since the closely spaced and similar modes are the lower bending modes in the N-S plane, this peculiar behavior conceivably results from the complicated interaction with the church, which is – in turn – determined by the shared load-bearing walls;

- The application of state-of-art algorithms of automated modal identification to the data continuously acquired through dynamic monitoring, allows accurate estimate and tracking of 4 modal frequencies;
- The resonant frequencies corresponding to the two lower modes f_{x1} and f_{y1} exhibit crossing in the hot season. This phenomenon, not observed so far in historic towers, results from the different effect exerted by the changing environment on the two frequencies. Furthermore, hybridization of the mode shapes is observed when the two natural frequencies become very close, as it happens in frequency veering rather than in the simpler frequency crossing;
- No significant changes were detected in the frequency statistics and in the frequency-temperature correlation during the monitoring period, suggesting that no appreciable change in the structural condition occurred;
- Despite the relatively limited number of identified frequencies, the PCA-based regression seems an effective tool to improve the automatically estimated frequencies by cleaning/mitigating the changes associated to the environmental effects.

ACKNOWLEDGEMENTS

The community of the Barnabite Order in Monza and Father R. Cagliani are gratefully acknowledged for the assistance during the field tests and the management/maintenance of the monitoring system.

REFERENCES

Allemang, R.J., and D.L. Brown 1982. A correlation coefficient for modal vector analysis. In *Proceedings of the 1st International Modal Analysis Conference (IMAC-I)*, 110-116. Orlando, USA. Society for Experimental Mechanics Inc.

Azzara, R.M., G. De Roeck, M. Girardi, C. Padovani, D. Pellegrini, and E. Reynders 2018. The influence of environmental parameters on the dynamic behaviour of the San Frediano bell tower in Lucca, *Engineering Structures* 156: 175-187. doi: 10.1016/j.engstruct.2017.10.045

Benedettini, F., D. Zulli, and R. Alaggio 2009. Frequency-veering and mode hybridization in arch bridges. In *Proceedings of the 27th International Modal Analysis Conference (IMAC-XXVII)*, Orlando, USA. Society for Experimental Mechanics Inc.

Binda, L., A. Saisi, and C. Tiraboschi 2000. Investigation procedures for the diagnosis of historic masonries, *Construction and Building Materials* 14(4): 199-233. doi: 10.1016/S0950-0618(00)00018-0

Brincker, R., L. Zhang, and P. Andersen. 2001. Modal identification of output-only systems using frequency domain decomposition, *Smart Materials and Structures* 10(3): 441-445. doi: 10.1088/0964-1726/10/3/303

Busatta, F. 2012. *Dynamic monitoring and automated modal analysis of large structures: methodological aspects and application to a historic iron bridge*. PhD Thesis, Politecnico di Milano.

Cabboi, A. 2013. *Automatic operational modal analysis: challenges and application to historic structures and infrastructures*. PhD Thesis, University of Cagliari.

Cabboi, A., F. Magalhães, C. Gentile, and A. Cunha 2017. Automated modal identification and tracking: application to an iron arch bridge, *Structural Control and Health Monitoring* 24(1), e1854. doi: 10.1002/stc.1854

Cantieni, R. 2014. One-year monitoring of a historic bell tower. In *Proceedings of the 9th international conference on structural dynamics*, *EURODYN 2014*, ed. À. Cunha, E. Caetano, P. Ribeiro, and G. Müller, 1477-1484. Porto, Portugal. European Association for Structural Dynamics.

Cavalagli, N., G. Comanducci, and F. Ubertini 2018. Earthquake-induced damage detection in a monumental masonry bell-tower using long-term dynamic monitoring data, Journal of Earthquake Engineering 22(Sup. 1): 96-119. doi: 10.1080/13632469.2017.1323048

Diaferio, M., D. Foti, and F. Potenza 2018. Prediction of the fundamental frequencies and modal shapes of historic masonry towers by empirical equations based on experimental data, *Engineering Structures* 156: 433-442. doi: 10.1016/j.engstruct.2017.11.061

Gentile, C., and A. Saisi 2007. Ambient vibration testing of historic masonry towers for structural identification and damage assessment, *Construction and Building Materials* 21(6): 1311-1321. doi: 10.1016/j.conbuildmat.2006.01.007

Gentile, C., A. Saisi, and A. Cabboi 2015, Structural identification of a masonry tower based on operational modal analysis, *International Journal of Architectural Heritage* 9(2): 98-110. doi: 10.1080/15583058.2014.951792

Gentile, C., M. Guidobaldi, and A. Saisi 2016. One-year dynamic monitoring of a historic tower: damage detection under changing environment, *Meccanica* 51: 2873-2889. doi: 10.1007/s11012-016-0482-3

Giannini, O., and A. Sestieri 2016. Experimental characterization of veering crossing and lock-in in simple mechanical systems, *Mechanical Systems and Signal Processing* 72-73: 846-864. doi: 10.1016/j.ymssp.2015.11.012

Jolliffe, I.T. 2002. *Principal component analysis*. New York: Springer.

Lorenzoni, F., M. Caldon, F. da Porto, C. Modena, and T. Aoki 2018. Post-earthquake controls and damage detection through structural health monitoring: applications in l'Aquila, *Journal of Civil Structural Health Monitoring* 8(2): 217-236. doi: 10.1007/s13349-018-0270-y

Lourenço, P.B. 2006. Recommendations for restoration of ancient buildings and the survival of a masonry chimney, *Construction and Building Materials* 20: 239-251. doi: 10.1016/j.conbuildmat.2005.08.026

Ljung, L. 1999. *System identification: theory for the user*. New Jersey: Prentice Hall.

Magnani Pucci, P., M. Colombo, and G. Marsili 1997. *The Church of Santa Maria di Carrobiolo* (in Italian). Monza: SPA Tipografica Sociale.

Mason, R.L., R.F. Gunst, and J.L. Hess 2003. *Statistical design and analysis of experiments with applications to engineering and science*. New York: John Wiley & Sons.

Oliveira, C.S., E. Çakti, D. Stengel, and M. Branco 2012. Minaret behavior under earthquake loading: the case of historical Istanbul, *Earthquake Engineering and Structural Dynamics* 41: 19-39. doi: 10.1002/eqe.1115

Peeters, B., and G. De Roeck 1999. Reference-based stochastic subspace identification for output-only modal analysis, *Mechanical Systems and Signal Processing* 13(6): 855-878. doi: 10.1006/mssp.1999.1249

Peña, F., P.B. Lourenço, N. Mendes, and D.V. Oliveira. 2010. Numerical models for the seismic assessment of an old masonry tower, *Engineering Structures* 32(5): 1466-1478. doi: 10.1016/j.engstruct.2010.01.027

Ramos, L.F., L. Marques, P.B. Lourenço, G. DeRoeck, A. Campos-Costa, and J. Roque 2010. Monitoring historical masonry structures with operational modal analysis: two case studies. *Mechanical Systems and Signal Processing* 24(5): 1291-1305. doi:10.1016/ j.ymssp.2010.01.011

Reynders, E., J. Houbrechts, and G. De Roeck 2012. Fully automated (operational) modal analysis, *Mechanical Systems and Signal Processing* 29: 228-250. doi: 10.1016/j.ymssp.2012.01.007

Saisi, A., C. Gentile, and A. Ruccolo 2018. Continuous monitoring of a challenging heritage tower in Monza, Italy, *Journal of Civil Structural Health Monitoring* 8(1): 77-90. doi: 10.1007/s13349-017-0260-5

Tomaszewska, A., and C. Szymczak 2012. Identification of the Vistola Mounting tower using measured modal data, *Engineering Structures* 42: 342-348. doi: 10.1016/j.engstruct.2012.04.031

Ubertini, F., G. Comanducci, N. Cavalagli, A.L. Pisello, A.L. Materazzi, and F. Cotana 2017. Environmental effects on natural frequencies of the San Pietro bell tower in Perugia, Italy, and their removal for structural performance assessment, *Mechanical Systems and Signal Processing* 82: 307-322. doi: 10.1016/j.ymssp.2016.05.025

Ubertini, F., N. Cavalagli, A. Kita, and G. Comanducci 2018. Assessment of a monumental masonry bell-tower after 2016 Central Italy seismic sequence by long-term SHM, *Bulletin of Earthquake Engineering* 16(2): 775-801. doi: 10.1007/s10518-017-0222-7

Table 1. Dynamic characteristics of the bell-tower identified from ambient vibration tests

Mode n.	Mode Identifier	f_{SSI} (Hz)	f_{FDD} (Hz)	D_f (%)	*MAC*
1	f_{x1} (E-W bending)	1.916	1.924	0.42	0.9997
2	f_{y1} (N-S bending)	2.011	2.012	0.05	0.9989
3	f'_{y1} (N-S bending)	2.367	2.363	0.17	1.0000
4	f_{y2} (N-S bending)	4.139	4.160	0.51	0.9748
5	f_{T1} (torsion)	4.554	4.570	0.35	0.9733
6	f_{T2} (torsion)	5.248	5.176	1.37	0.9883
7	f_{x2} (E-W bending)	7.528	7.539	0.15	0.9783

Table 2. Correlation coefficients between the temperatures measured from 22/10/2015 to 21/10/2016

	T_{0N}	T_{1E}	T_{2E}	T_{2W}	T_S
T_{0N}	1.000	0.967	0.957	0.960	0.837
T_{1E}		1.000	0.995	0.997	0.873
T_{2E}			1.000	0.998	0.900
T_{2W}				1.000	0.885
T_S					1.000

Table 3. Statistics of the natural frequencies identified during the first and the second year of monitoring

Mode Identifier	f_{ave} (Hz)		σ_f (Hz)		f_{min} (Hz)		f_{max} (Hz)	
	1st Year	2nd Year	1st Year	2nd Year	1st Year	2nd Year	1st Year	2nd Year
f_{x1}	1.946	1.951	0.041	0.046	1.876	1.852	2.094	2.100
f_{y1}	2.020	2.100	0.009	0.010	1.990	1.970	2.053	2.057
f^*_{y1}	2.379	2.377	0.015	0.017	2.333	2.314	2.423	2.443
f_{T2}	5.265	5.274	0.141	0.124	5.001	4.972	5.663	5.677

Table 4. Performance of the frequency prediction obtained using the MLR and the PCA-based regression (training period, from 22/10/2015 to 21/10/2016)

	R^2		ρ_{xy}		*LF*	
	MLR	PCA	MLR	PCA	MLR	PCA
f_{x1}	0.883	0.937	0.934	0.968	2.12 E-04	9.36 E-05
f_{y1}	0.464	0.935	0.651	0.967	4.79 E-05	5.23 E-06
f^*_{y1}	0.560	0.896	0.737	0.946	1.10 E-04	2.37 E-05
f_{T2}	0.856	0.928	0.923	0.963	2.93 E-03	1.18 E-03

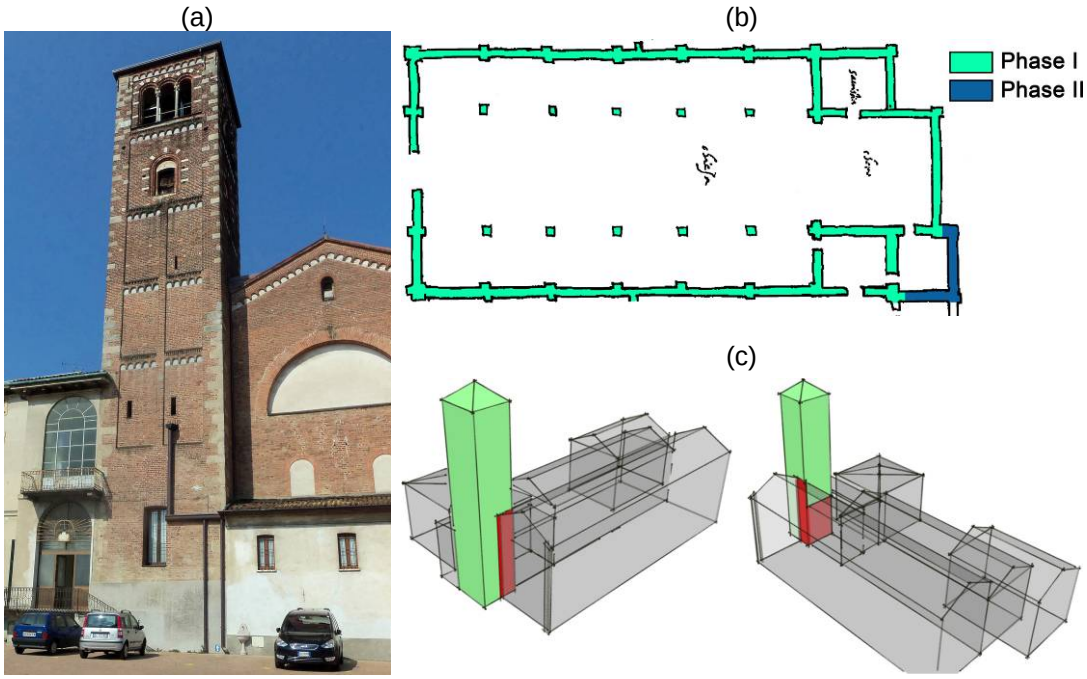

Figure 1. The church of *Santa Maria del Carrobiolo* and the bell-tower (Monza, Italy):
(a) East view; (b) Building evolution in a plan dating back to 1572; (c) Axonometric representation of the interaction between the church and the tower.

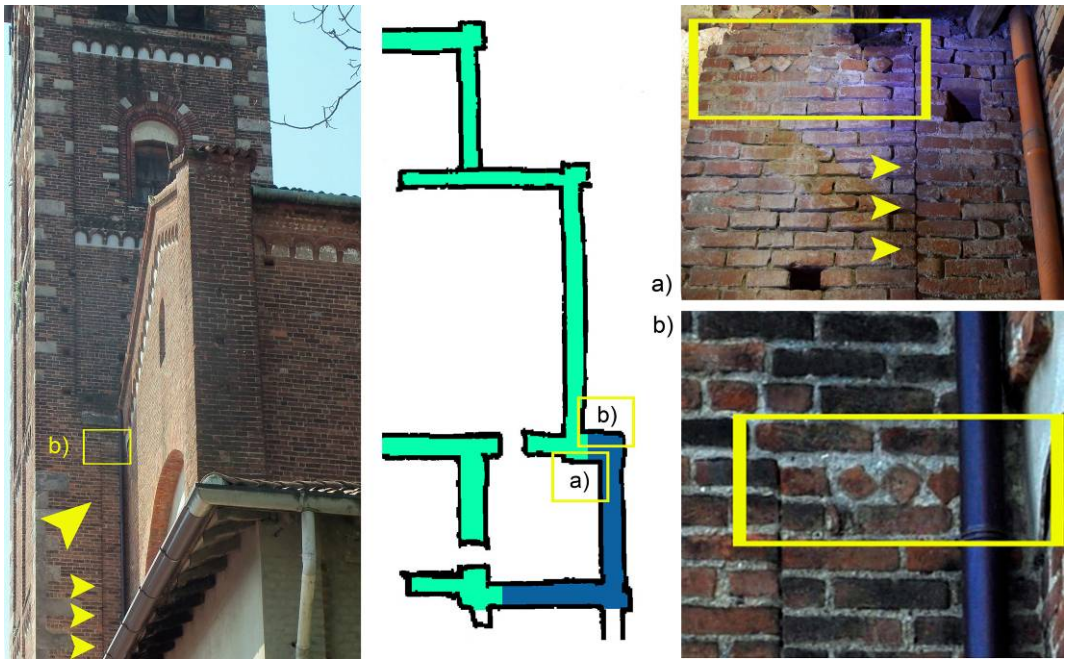

Figure 2. Structural discontinuities due to the building phases.

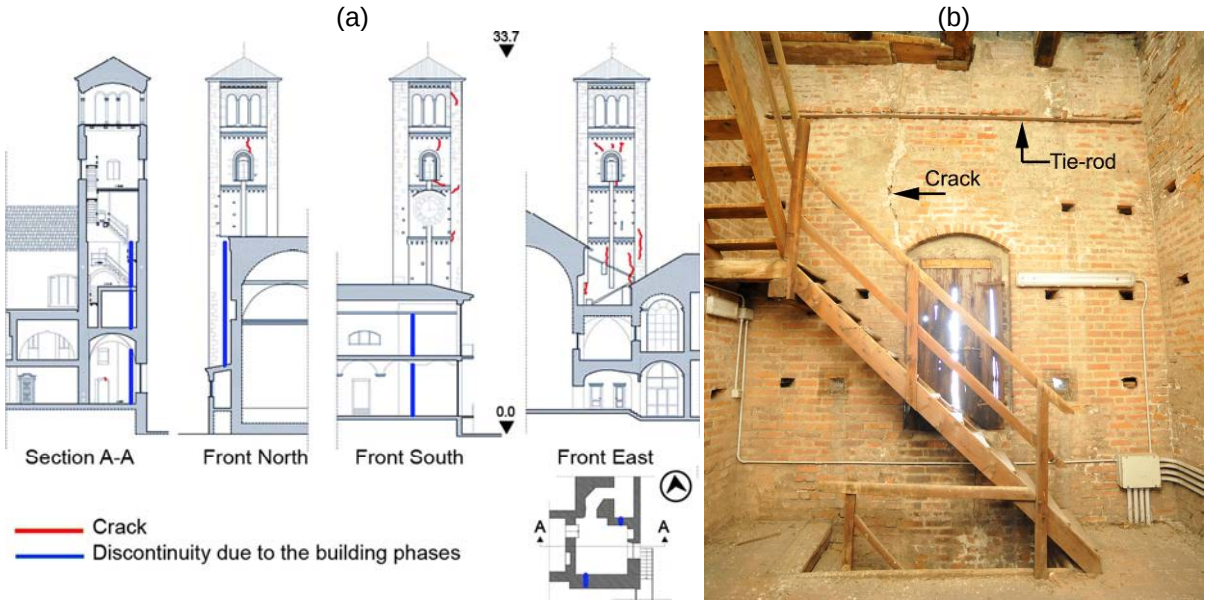

Figure 3. (a) Geometric and crack pattern surveys of the bell-tower; (b) Metallic tie-rod installed below the belfry (Level 2, West side).

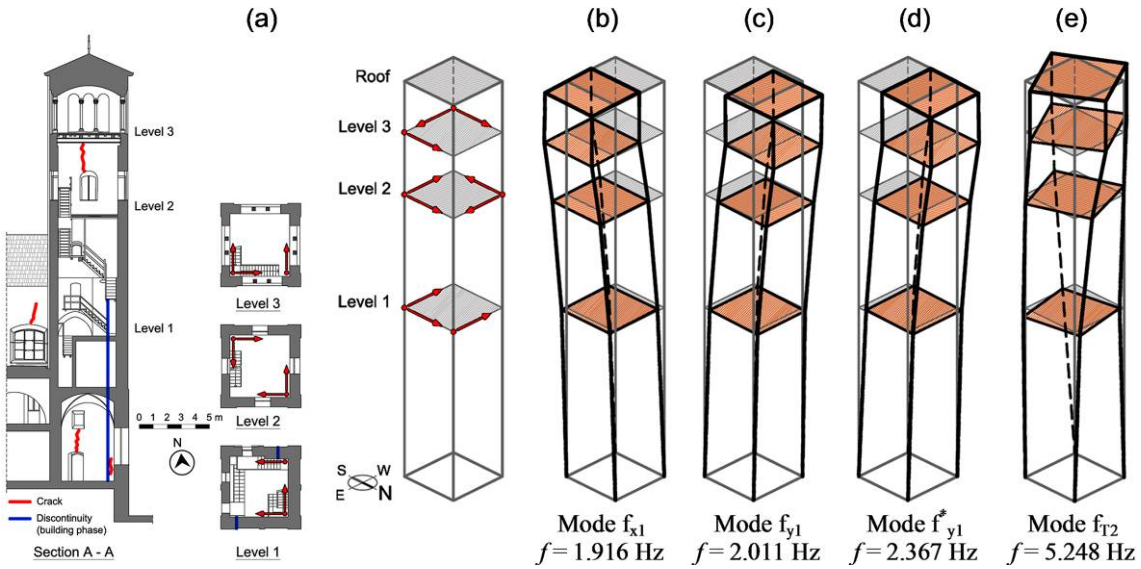

Figure 4. Ambient vibration tests: (a) Schematic of the sensors layout; (b-e) Selected modes of vibration identified from operational modal analysis (SSI-Cov).

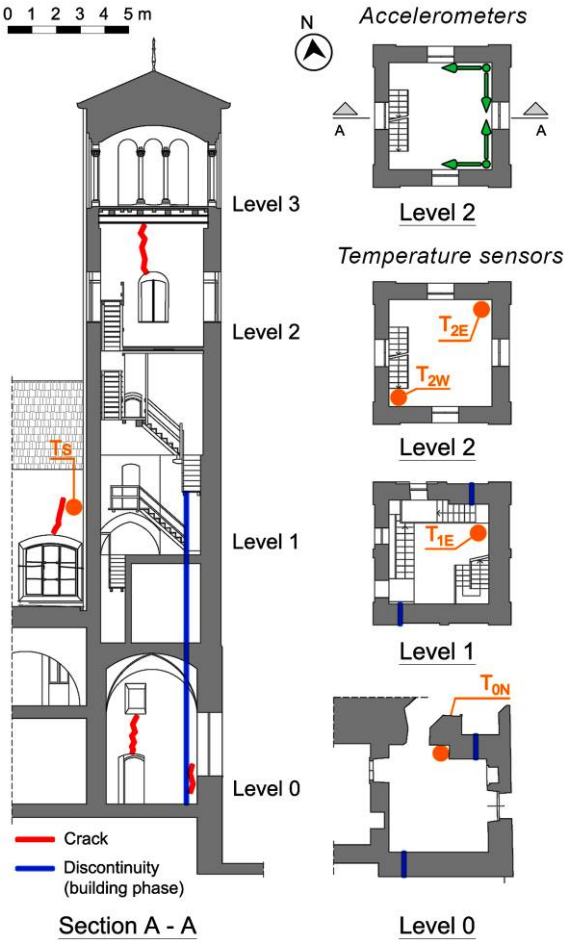

Figure 5. Continuous monitoring: layout of the installed sensors.

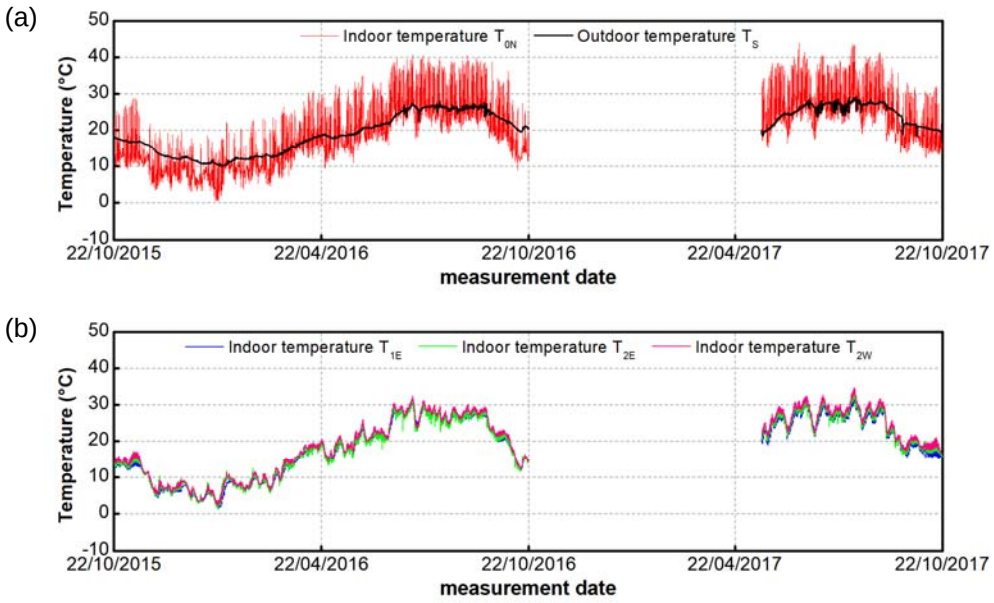

Figure 6. Variation in time of measured temperatures (from 22/10/2015 to 21/10/2017): (a) T_{0N} and T_S; (b) T_{1E}, T_{2E} and T_{2W}.

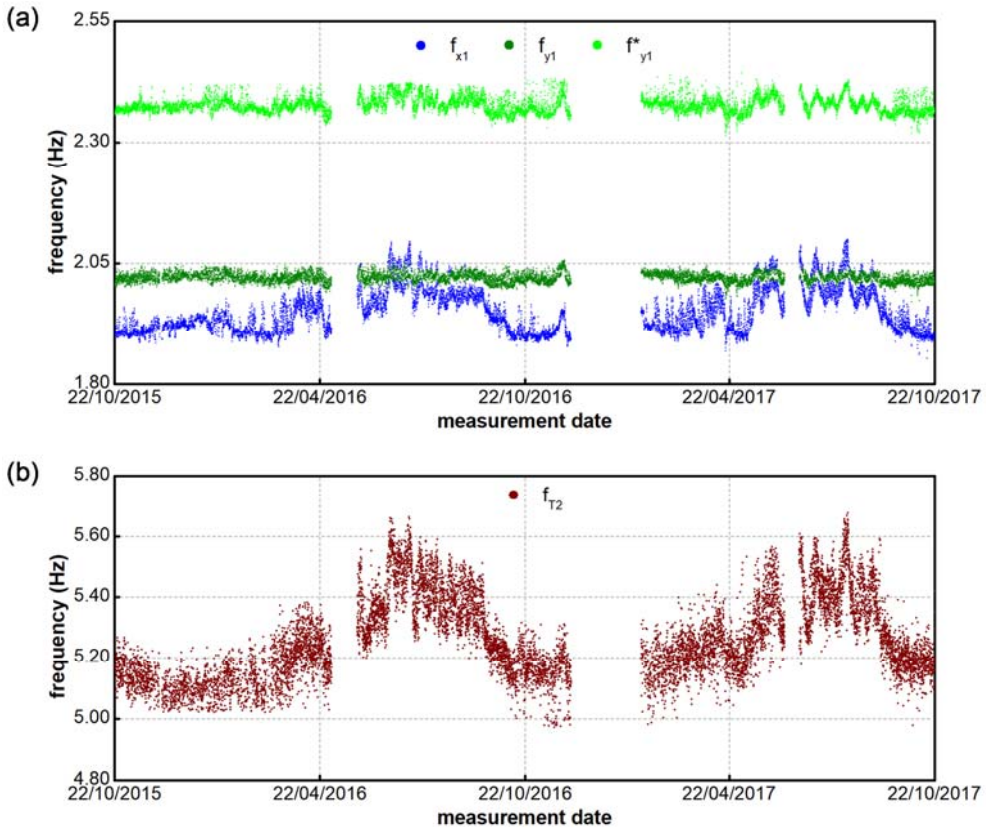

Figure 7. Variation in time of the automatically identified natural frequencies (from 22/10/2015 to 21/10/2017): (a) modes f_{x1}, f_{y1} and f^*_{y1}; (b) mode f_{T2}.

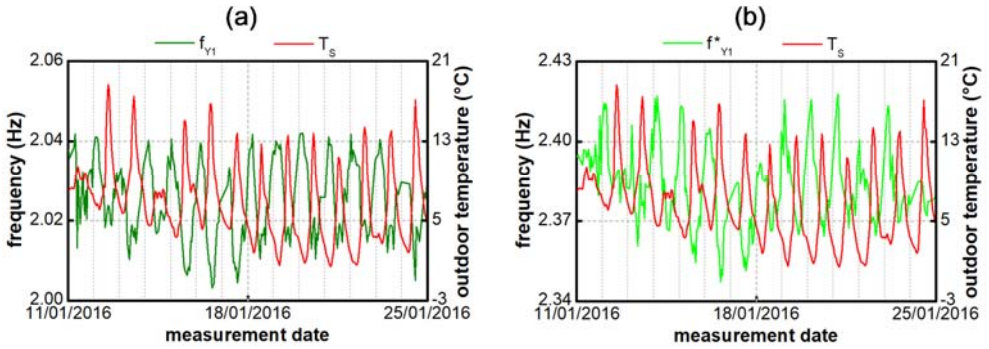

Figure 8. Typical variation of the outdoor temperature and natural frequency in Winter: (a) mode f_{y1}; (b) mode f^*_{y1}.

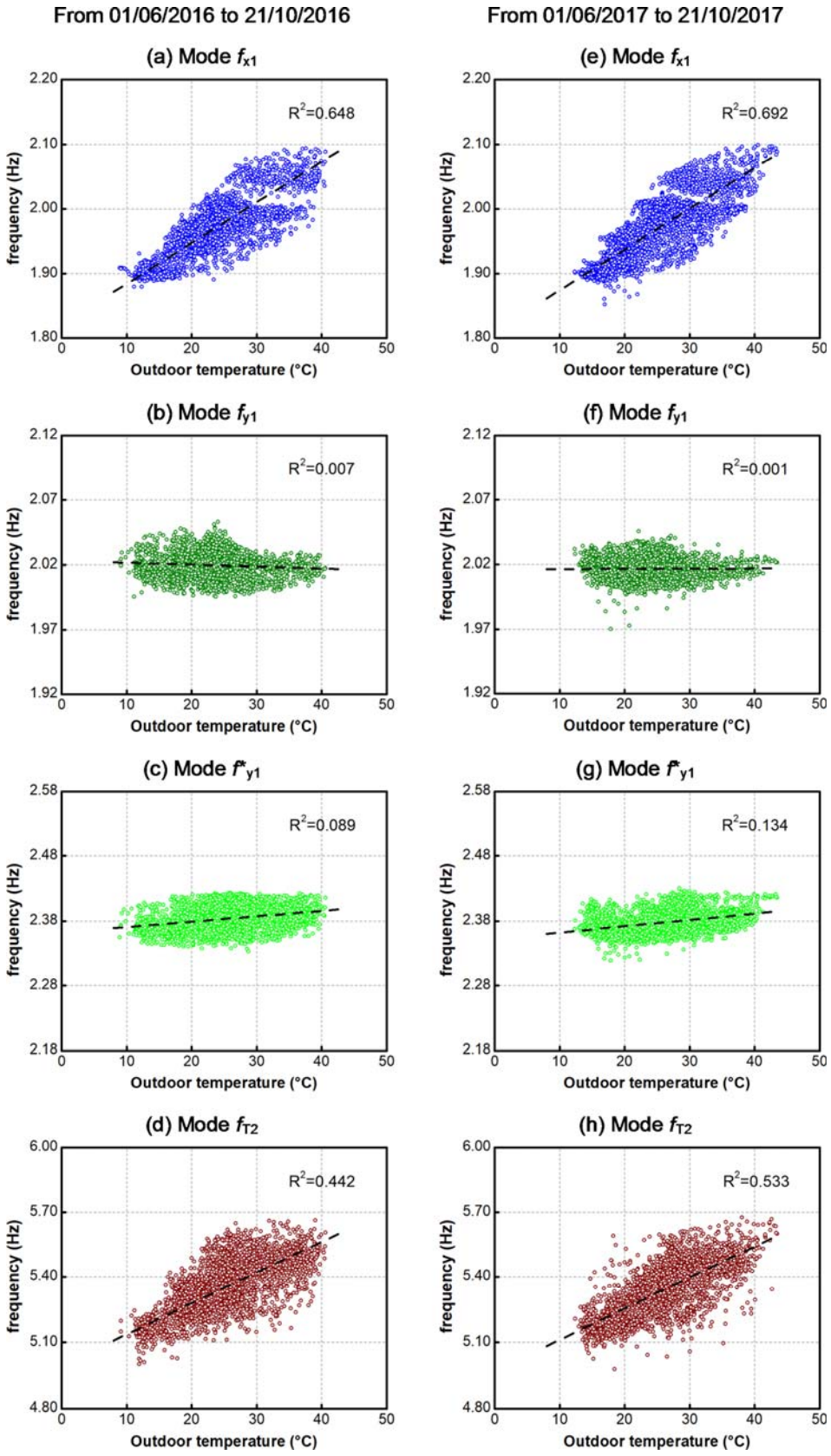

Figure 9. Natural frequency of modes f_{x1}, f_{y1}, f^*_{y1} and f_{T2} plotted versus the outdoor temperature: (a-d) from 01/06/2016 to 21/10/2016 and (e-h) from 01/06/2017 to 21/10/2017.

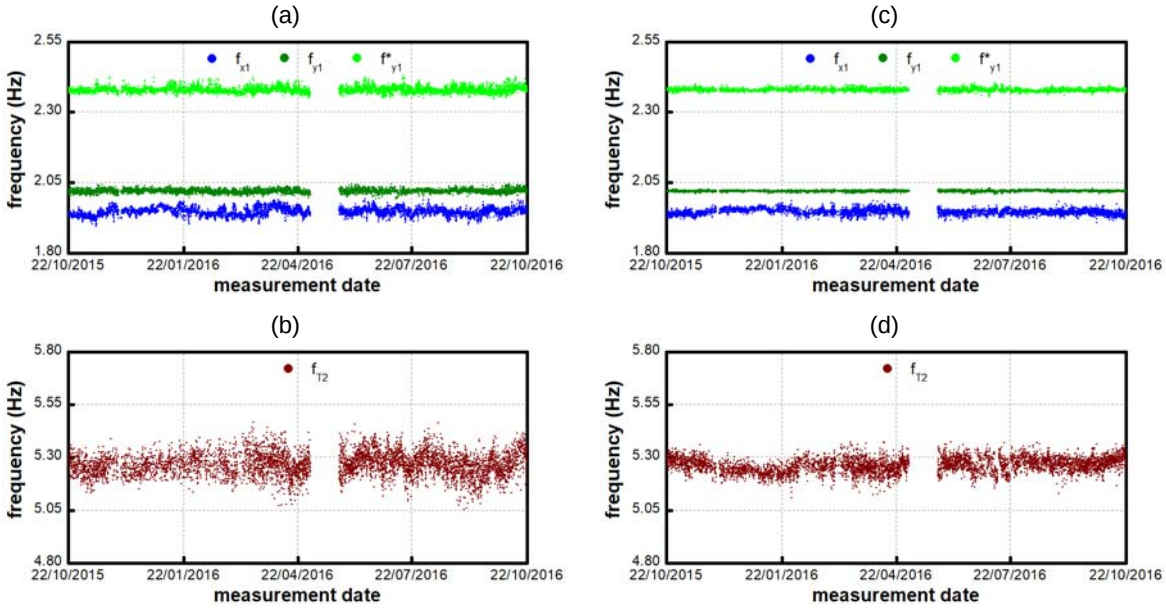

Figure 10. Time evolution of the cleaned modal frequencies (from 22/10/2015 to 21/10/2016) after applying the MLR (a-b) and the PCA-based regression (c-d) to mitigate variability due to changes in the environment.

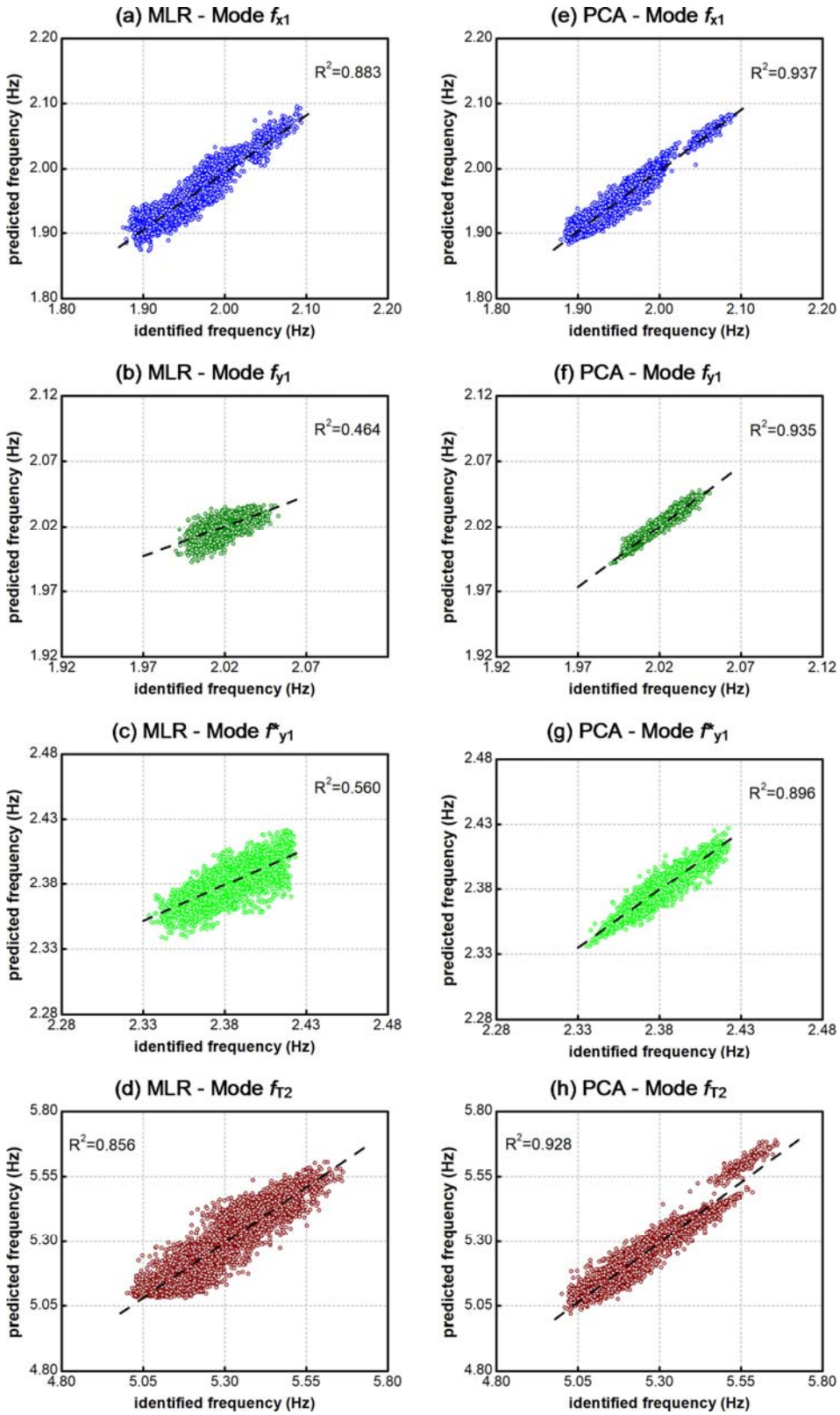

Figure 11. Correlation between the identified frequencies (from 22/10/2015 to 21/10/2016) and the ones predicted by applying the MLR (a-d) and the PCA-based (e-h) regression.

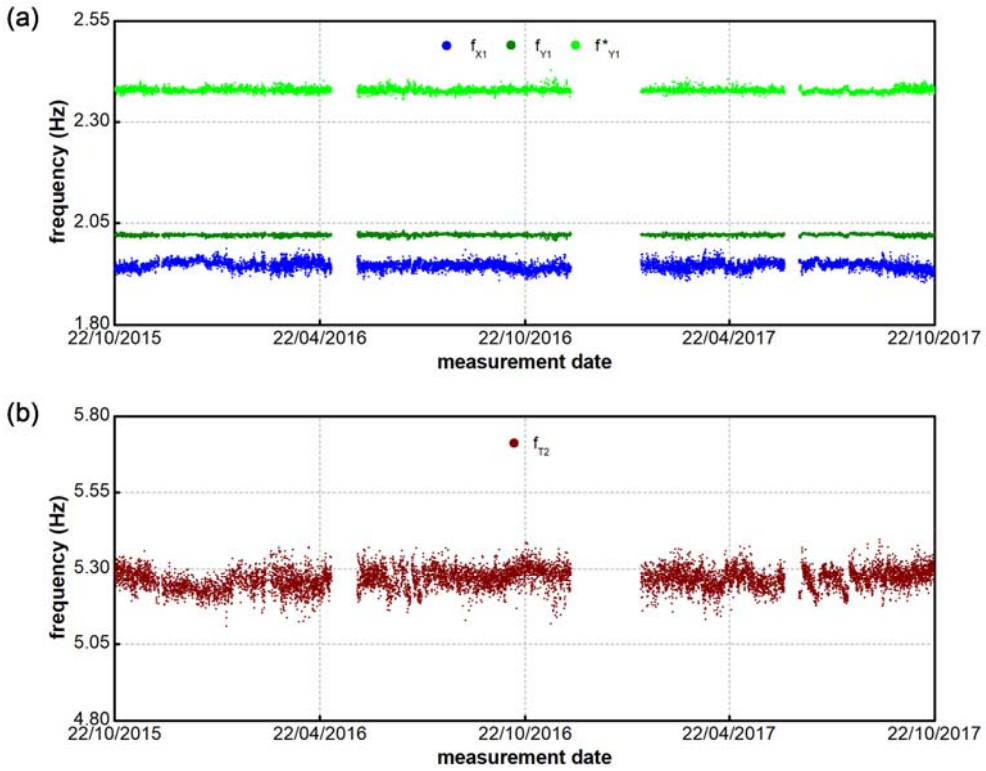

Figure 12. Time evolution of the cleaned (PCA-based regression) modal frequencies from 22/10/2015 to 21/10/2017: (a) modes f_{x1}, f_{y1} and f^*_{y1}; (b) mode f_{T2}.